RESEARCH ARTICLE

Terra Nova WILEY

A frozen oceanic crystal mush

V. Basch[1,2] | C. Ferrando[2,3] | A. Sanfilippo[1,2]

[1]CNR-Istituto di Geoscienze e Georisorse, Pavia, Italy

[2]University of Pavia, DSTA, Pavia, Italy

[3]University of Genoa, DISTAV, Genoa, Italy

Correspondence
Valentin Basch, CNR-Istituto di Geoscienze e Georisorse, Via Ferrata 1, Pavia 27100, Italy.
Email: valentin.basch@gmail.com

Abstract

The processes driving the evolution of crystal mushes are often documented in complex systems where crystallization, assimilation, magma replenishment and mixing occur concurrently and are generally overprinted by compaction and deformation. Documenting the characteristics of an undisturbed crystal mush is thus of upmost importance; it highlights the initial conditions with which complex crystal mush processes proceed. We here present the structure and composition of an oceanic crystal mush through detailed petro-structural and chemical study of metre-scale intrusions from the Mid-Atlantic Ridge. Textures, bulk-rock and mineral compositions indicate closed-system crystallization of primitive melts, undisturbed by dissolution–precipitation reactions and subsequent deformation. These frozen crystal mushes record the simplest possible evolution of small-scale intrusions and can be used as a baseline to pinpoint the impact of crystal mush processes on the evolution of complex systems. Any divergence from this reference results from processes occurring concomitantly to the progressive closure of the magmatic system.

KEYWORDS
crystal growth, crystal mush baseline, fractional crystallization, magma chamber, oceanic lower gabbros

1 | INTRODUCTION

The magmatic processes that contribute to the accretion of the oceanic and continental crust mainly take place in crustal magma chambers (e.g., Cashman et al., 2017). Although the latter have long been considered as melt-dominated reservoirs, accumulating geophysical and petrological evidence called for a revision of the conceptual model of magma chambers (see Edmonds et al., 2019; White et al., 2019 for a review). The new paradigm envisions magma reservoirs as crystal mushes filled with variable proportions of crystals and interstitial melt (e.g., Cashman et al., 2017; Cooper, 2017; Lissenberg et al., 2019). Multiple processes have been documented to occur within crystal mushes, namely crystallization, assimilation, magma replenishment and mixing (e.g., Coogan & Dosso, 2016;

Lissenberg et al., 2019; Namur et al., 2013; Tegner et al., 2009), often overprinted by successive compaction and solid-state plastic deformation (e.g., Bertolett et al., 2019; Cheadle & Gee, 2017; Ferrando, Basch, et al., 2021; Holness et al., 2017; Meurer & Boudreau, 1998). Each of these processes has profound implications on the chemical evolution of magmatic systems and may control the style of melt migration, extraction, and eruption (e.g., Jackson et al., 2018; Lissenberg et al., 2019; Sparks et al., 2019).

This contribution focuses on mid-ocean ridge systems, where percolation of primitive mid-ocean ridge basaltic (MORB) melts within the mushy gabbroic crust is driven by melt buoyancy and possibly enhanced by compaction, either gravity- or deformation-related (e.g., Basch, Sanfilippo, Vigliotti, et al., 2022; Ferrando, Basch, et al., 2021; Lissenberg et al., 2019; McKenzie, 1984). Throughout

these crystal mushes, the chemical composition of tholeiitic melts is ubiquitously modified by several magmatic processes, such as: (i) partial crystallization of primitive mineral phases, which leads to progressive enrichment in the melt trace element contents, (ii) dissolution–precipitation reactions between the melt and the percolated gabbroic mush, leading to specific enrichments in highly incompatible trace elements, as commonly evidenced by strong fractionation between Light (L-) and Heavy Rare Earth Elements (H-REE) from core to rim of clinopyroxene crystals (e.g., Basch, Sanfilippo, Skolotnev, et al., 2022; Ferrando, France, et al., 2021; Lissenberg & MacLeod, 2016; Sanfilippo et al., 2020; Zhang et al., 2020), (iii) replenishment and mixing with migrating melts having different chemical compositions, in turn generating hybrid melts, as displayed by complex zoning patterns in crystallized phases (i.e., Coogan & Dosso, 2016; Coumans et al., 2016; Leuthold et al., 2018; Moore et al., 2014). However, because these processes can occur concomitantly, deciphering the impact of a single magmatic process within such complex systems is not trivial. To constrain the evolution of oceanic crystal mushes and properly document the contribution of each process on their chemical composition, we currently lack knowledge on the initial chemical signature of a primitive crystal mush. In this contribution, we document a "baseline" of basaltic crystal mush, that is, the composition and texture of an undeformed crystal mush that solely involved fractional crystallization within a closed magmatic system, and therefore did not suffer dissolution–precipitation processes, magma replenishment and mixing, nor subsequent deformation. We study metre-scale oceanic dolerites recording crystallization of small-scale magmatic intrusions within the oceanic crust. This crystal mush ought to serve as reference to constrain the early evolution of the tholeiitic intrusions building the lower oceanic crust. The limited dimension of these basaltic intrusions impeded compaction and chemical interaction with exotic melts, thereby providing a proxy of an undeformed crystal mush that did not suffer any chemical modification.

2 | SAMPLE SELECTION AND RESULTS

The selected oceanic dolerites are interpreted as metre-scale magmatic intrusions within the lower oceanic crust formed at the Mid-Atlantic ridge. We chose eight samples recovered from a lower crustal section exposed at an Oceanic Core Complex located at 8.1°N along the Mid-Atlantic Ridge within the Doldrums Fracture Zone (Basch, Sanfilippo, Skolotnev, et al., 2022; Skolotnev et al., 2020). Petrographic descriptions have been accompanied by Electron Back-Scatter Diffraction (EBSD) analyses, and bulk-rock and mineral major and trace element analyses. Methodologies are detailed in the Data S1.

Samples are characterized by a millimetre-sized doleritic texture of euhedral plagioclase laths (63–66 vol%), granular olivine (6–7 vol%) and minor Fe-Ti oxide (2 vol%; ilmenite and magnetite), embedded in poikilitic clinopyroxene (26–29 vol%) up to centimetre in size (Figure 1a,b; Figure S1). At the thin section scale, all samples present

Statement of significance

We here document the structure and geochemical composition of a frozen basaltic crystal mush, using oceanic metre-scale intrusions as a proxy of uncompacted crystal mushes that evolved exclusively by fractional crystallization in a closed system. This frozen crystal mush records the simplest possible evolution of an oceanic magmatic chamber and can be used as a reference to pinpoint the impact of crystal mush processes on the structural and chemical evolution of more complex systems. The main implication of this study is that structural and chemical divergence from this undisturbed oceanic crystal mush must be attributed to additional processes occurring concomitantly to the progressive closure of the magmatic system. This contribution is one of the missing pieces of the crystal mush puzzle and we believe that it will be of interest to the scientific community studying igneous petrology of the lower oceanic crust.

a patchy texture, with millimetre- to centimetre-sized troctolitic areas composed of mainly euhedral olivine and plagioclase, and areas composed of clinopyroxene oikocrysts including plagioclase and Fe-Ti oxide (ilmenite and magnetite) chadacrysts (Figure 1a,b). EBSD investigations show that all phases are undeformed, with even the largest plagioclase laths showing less than 2° misorientation of its crystallographic network (Figure 1c). Olivine and plagioclase show no Crystallographic Preferred Orientation (CPO) but rather random orientations (i.e., no CPO pattern, J-index ~1–1.5; Figure 1d,e).

Olivine (Table S1) shows strongly variable Forsterite (Fo = 63.7–88.6 mol%) and NiO contents (0.06–0.26 wt%) (Figure 2a; Figure S2). Plagioclase (Table S2) shows Anorthite contents varying in a wide chemical range from 10.3 to 86.8 mol%, and FeO contents range between 0.22 and 0.92 wt% (Figure 2b; Figure S3). Such strong chemical variability can be observed at the scale of a single crystal, with plagioclase cores systematically displaying primitive compositions (An ~70–80 mol%), whereas the rims show more evolved compositions (An ~20–40 mol%) (Figure 3; Figure S4). Similar to olivine and plagioclase, clinopyroxene (Table S3) shows strong chemical variability, with Mg-numbers varying from 53.8 to 83.9 mol% and TiO_2 contents varying between 0.51 and 1.46 wt% (Figure 2c). Notably, the core-to-rim chemical variability of poikilitic clinopyroxene is less systematic than that of plagioclase crystals. Taken as a whole, plagioclase-olivine and plagioclase-clinopyroxene mineral couples show positive correlation of Fo-An-Mg#$_{cpx}$ (Figure 2a,b), encompassing the entire chemical variability documented in the Atlantis Massif OCC lower oceanic crust, along the Mid-Atlantic Ridge (Figure S2; Figure S3; Miller et al., 2009).

Bulk-rock compositions of the selected samples reveal a primitive character (Table S4), with Mg-numbers (Mg# = Mg/[Mg + Fe] mol%) ranging from 65.1 to 73.4 mol% (average of 70.5 mol%),
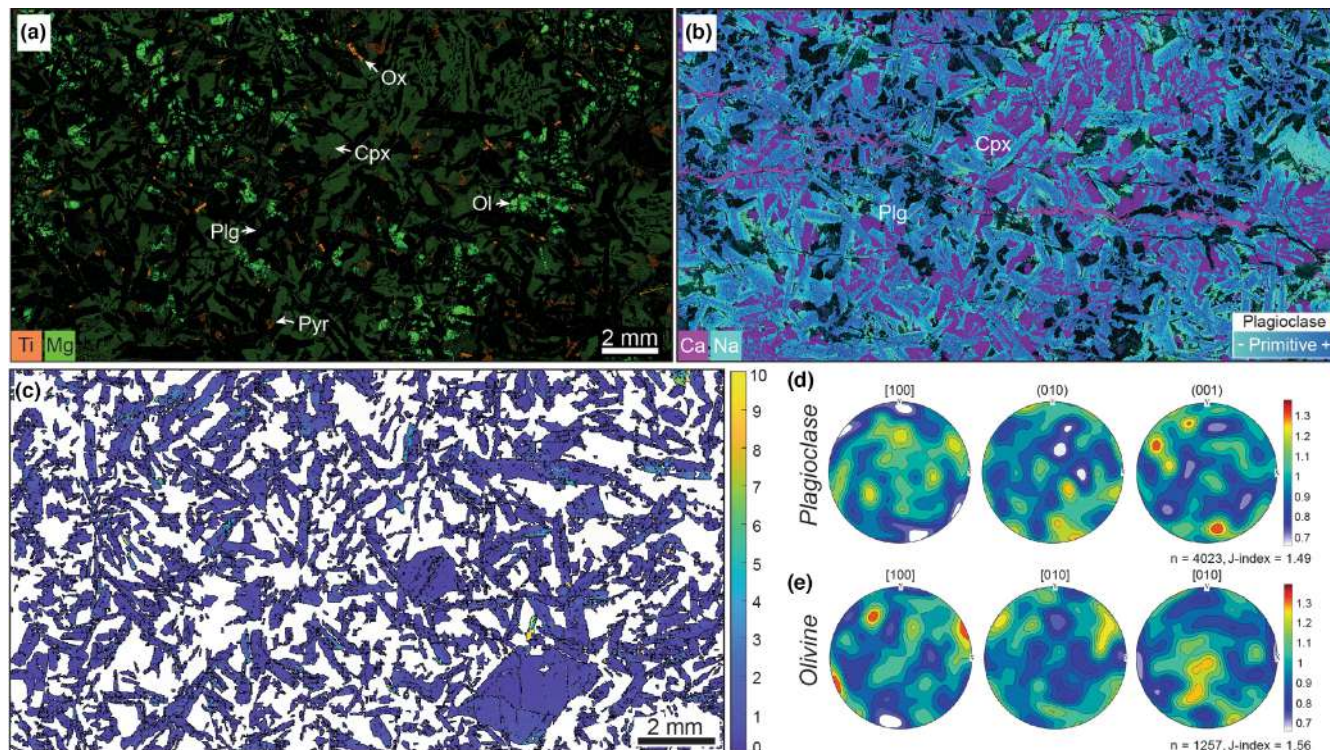
FIGURE 1 Representative texture of the studied doleritic gabbros. (a) Stacked Energy Dispersive Spectrometry (EDS) chemical maps of Ti and Mg, evidencing the patchy occurrence of olivine (green). (b). Stacked EDS maps of Ca and Na, evidencing the evolved character of plagioclase crystals (light blue) associated with clinopyroxene chadacrysts (purple). (c) Plagioclase Mis2Mean map (misorientation of single pixels respect to the mean orientation of the crystal) of the doleritic texture, evidencing undeformed plagioclase (colour bar from 0° to 10°). (d, e) One-point-per-grain equal-area, lower hemisphere stereographic projections of the Crystallographic Preferred Orientation of plagioclase (d) and olivine (e). The colour bar is scaled to the maximum concentration of the three crystallographic axes. [Colour figure can be viewed at wileyonlinelibrary.com]

and Ca-numbers (Ca#=Ca/[Ca+Na] mol%) ranging from 62.1 to 72.0 mol% (average of 68.9 mol%; Figure 2d). These ratios, together with low TiO_2 (0.86–1.46 wt%; Figure 2e) and Na_2O contents (2.2–3.1 wt%), and high Al_2O_3 (14.2–17.2 wt%), MgO (9.8–12.1 wt%) and CaO contents (9.2–10.5 wt%), plot at the most primitive end of the global Mid-Ocean Ridge Basalt (MORB) database (Gale et al., 2013). Consistently, the bulk-rock trace element compositions show Rare Earth Element (REE) patterns (Table S1) similar to primitive N-MORB compositions (Workman & Hart, 2005), with overall low REE contents (e.g., Yb_N=11.9–12.0; N=normalized to CI chondrite from Sun & McDonough, 1989) showing relatively flat patterns slightly depleted in LREE (Ce_N/Yb_N=0.82–0.83) and no Eu anomalies (Figure 2f).

3 | CLOSED-SYSTEM EVOLUTION AND CRYSTAL GROWTH

The texture characterizing the dolerites suggests that no compaction nor solid-state deformation affected the samples during and after their crystallization (Bertolett et al., 2019; Cheadle & Gee, 2017; Ferrando, Basch, et al., 2021). The random orientation of olivine and plagioclase testifies to crystal suspension within a static and initially

melt-supported crystal mush (e.g., Ildefonse et al., 1992, 1997). Furthermore, the occurrence of more primitive troctolitic areas embedded within a more evolved matrix indicates that initial crystal nucleation and growth were neither homogeneously distributed within the metre-sized intrusion, nor concentrated on the walls of the magmatic chamber (e.g., Tegner et al., 2009); rather, it proceeded within melt-suspended primitive patches (Figure 1a). The absence of flow-driven lineation (Figure 1d) within these patches also argues against the occurrence of antecrysts, which would have been oriented during magmatic flow and emplacement of the intrusion, in turn indicating that all crystals formed after emplacement of the metre-scale intrusions. These textures are consistent with slow-spreading ridge settings, in which the small dimension of crystal mushes hampers gravity-driven compaction, extensive magmatic flow leading to sorting and alignment of the crystals and favours static cooling of the intrusion (e.g., Cheadle & Gee, 2017).

In agreement with these textures, the bulk-rock compositions of all samples do not correspond to cumulate gabbros typically showing positive Eu anomalies, but instead to primitive melts that did not suffer any melt extraction (e.g., Godard et al., 2009). Consistently, our dolerite samples contain all the phases expected along the liquid line of descent of a tholeiitic melt (e.g., Grove et al., 1992; Villiger et al., 2007), from liquidus (olivine) to near-solidus temperatures
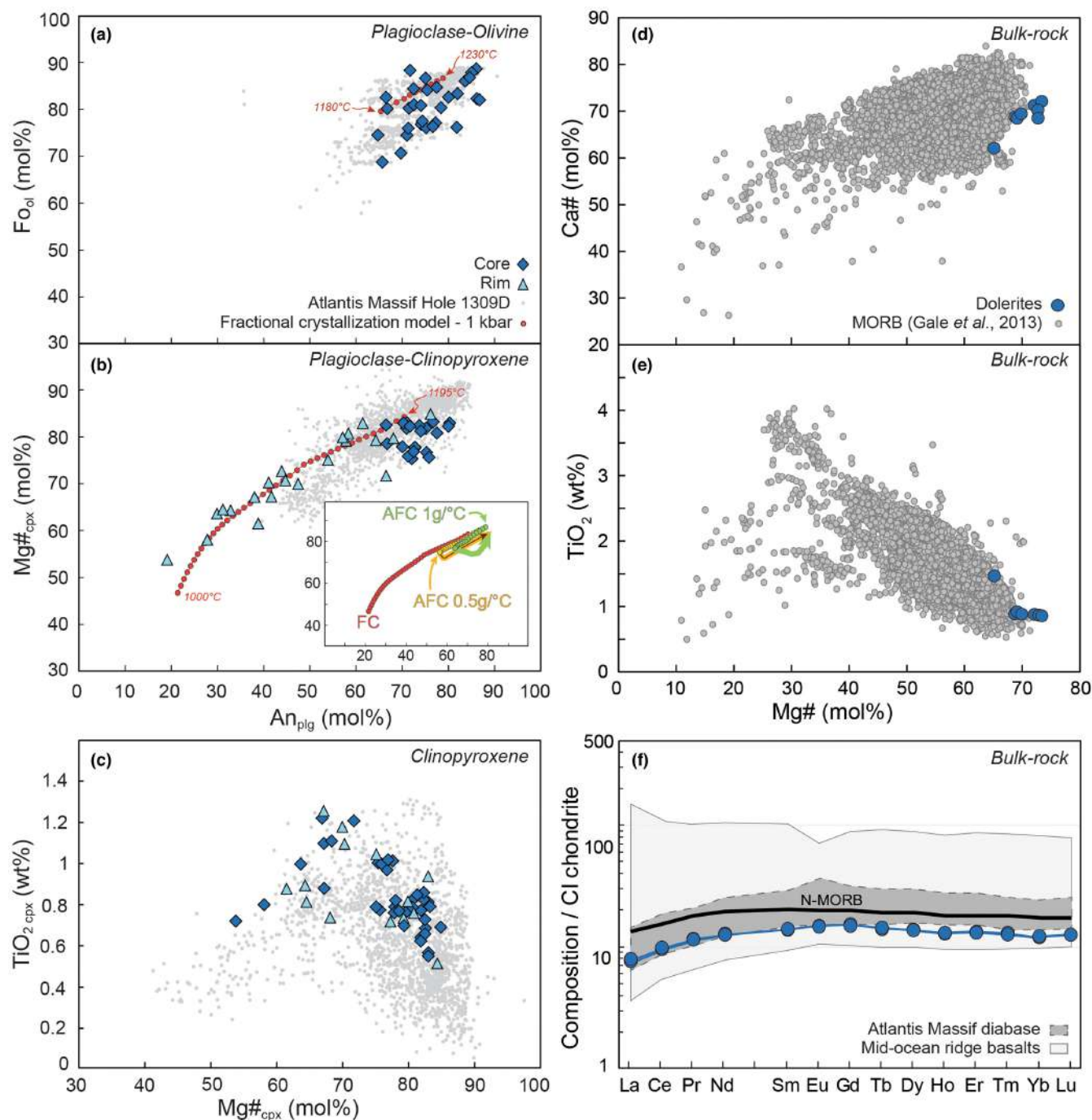
FIGURE 2 Mineral and bulk-rock compositions of the studied doleritic gabbros. (a) Anorthite content (plagioclase) vs. Forsterite content (olivine). (b) Anorthite content (plagioclase) vs. clinopyroxene Mg# (100 x cationic Mg/[Mg + Fe] mol%). (c) Clinopyroxene Mg# vs. TiO_2. (d) Bulk-rock Mg# vs. Ca# (100 x cationic Ca/[Ca + Na] mol%). (e) Bulk-rock Mg# vs. TiO_2. (f) CI chondrite-normalized bulk-rock REE patterns. Normalization values after Sun and McDonough (1989). The mineral compositions from the Atlantis Massif Hole 1309D gabbros and diabases (Miller et al., 2009) and the global MORB database from Gale et al. (2013) are plotted for comparison. Also shown is the fractional crystallization model of the average composition of dolerites (after Workman & Hart, 2005) at 1 kbar, using the MELTS thermodynamic software (Ghiorso & Sack, 1995). The inset in B compares the MELTS models of fractional crystallization (FC) to the assimilation-fractional crystallization (AFC) paths involving 0.5 and 1 g/°C dissolution of a primitive olivine gabbro (ol:plg:cpx = 0.2:0.5:0.3). [Colour figure can be viewed at wileyonlinelibrary.com]

(ilmenite, magnetite; Figure 1a,b). At the scale of the thin section, the most zoned and evolved plagioclase crystals (light blue areas in Figure 1b) are associated with clinopyroxene oikocrysts in the areas

lacking olivine and bearing Fe-Ti oxides (dark green areas in Figure 1a), thus corresponding to the last crystallized portions. Textures and chemistry therefore indicate that the studied metre-scale intrusions
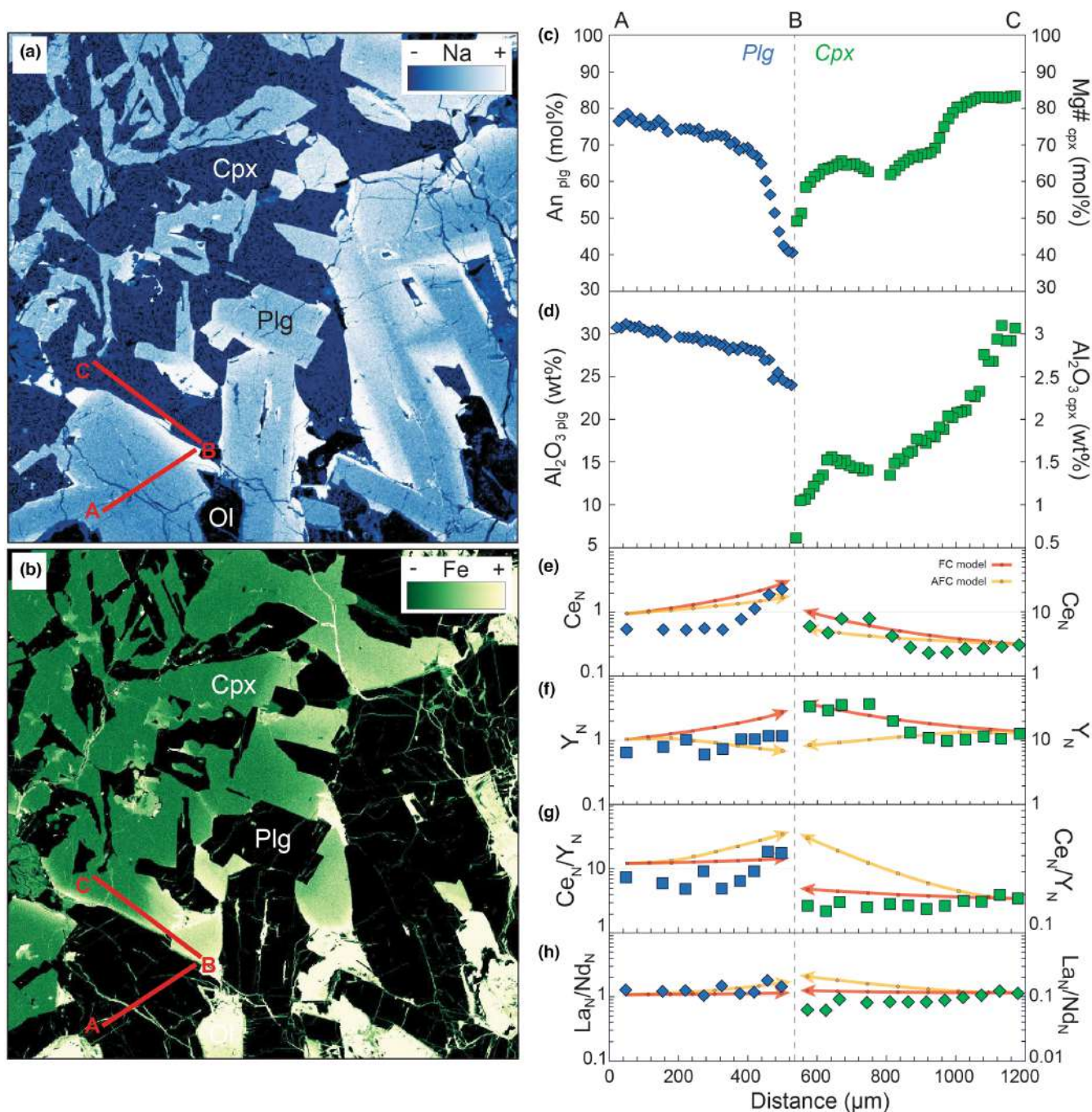
FIGURE 3 Chemical maps and profiles. (a) Detailed EDS map of Na, evidencing chemical zoning of the plagioclase crystals. (b) Detailed EDS map of Fe, evidencing chemical zoning of clinopyroxene crystals. Red lines indicate the location of the A-B-C chemical profile. (c) Anorthite (plagioclase) - Mg# (clinopyroxene) chemical profile from plagioclase core to clinopyroxene core. (d) Al_2O_3 chemical profile. (e) Ce_N chemical profile. (f) Y_N chemical profile. (g) Ce_N/Y_N chemical profile. (h) La_N/Nd_N chemical profile. Normalization values after Sun and McDonough (1989). The yellow line represents the computed chemical profile of crystal growth involving assimilation of a gabbroic crystal mush upon melt crystallization (AFC), while the red line corresponds to the chemical profile resulting from simple fractional crystallization (FC). [Colour figure can be viewed at wileyonlinelibrary.com]

are representative of the closed-system evolution of a crystal mush, from the initial crystallization of euhedral olivine and An-rich plagioclase within the troctolitic patches at temperatures close to the liquidus, to the crystallization of An-poor plagioclase, clinopyroxene and Fe-Ti oxides at gradually decreasing temperatures (see Dick et al., 2002; Feig et al., 2006; Villiger et al., 2007).

Although the intrusions are characterized by primitive bulk-rock compositions, minerals show strong core-to-rim chemical variations within single plagioclase and clinopyroxene crystals. The latter show decreasing Anorthite_plg, Mg#_cpx and Al_2O_3 contents, and increasing incompatible trace element contents from core to rim of the crystals (Figure 3). Notably, reactive processes such as

the dissolution of primitive gabbroic mushes would lead to a buffer of the major elements towards primitive compositions (see inset in Figure 2b; detail of the thermodynamic models is given in the Data S1), which is in contrast with the documented linear mineral chemical variations. Furthermore, no strong fractionation is observed between highly to less incompatible elements during progressive growth of plagioclase and clinopyroxene crystals (Figure 3f; Figure S4), as it would be expected during dissolution-precipitation reactions (Figure 3e-h; e.g., Ferrando, France, et al., 2021; Leuthold et al., 2018; Lissenberg & MacLeod, 2016; Sanfilippo et al., 2020; Sparks et al., 2019). Conversely, the dolerite mineral chemical co-variations follow fractional crystallization paths at 1 kbar from primitive to evolved compositions (MELTS models; Figure 2a,b; Ghiorso & Sack, 1995). The normal zoning denoted by major and trace element chemical profiles through plagioclase-clinopyroxene contacts (Figure 3; Figure S4; Table S5), together with the crystal growth patterns (e.g., Smith & Lofgren, 1983), developed during the progressive cooling and closure of the magmatic system. This is in line with a simple process of closed-system fractional crystallization (FC) of a primitive parental melt, with no involvement of replenishment, mixing or reactive processes. Ultimately, the growth patterns of poikilitic clinopyroxene correspond to the closure of the porosity, "locking" the crystal mush at temperatures close to the solidus.

4 | AN UNDISTURBED CRYSTAL MUSH

The texture and compositions characterizing the studied small-scale intrusions provide important constraints on the petrological evolution of a tholeiitic crystal mush during progressive cooling. Namely, crystallization initiated heterogeneously within the intrusion, forming primitive areas of euhedral olivine and plagioclase oriented randomly (Stage 1 in Figure 4). Upon cooling, crystal growth dominated within the primitive areas, while clinopyroxene started to nucleate together with plagioclase within the crystal-poor areas (Stage 2 in Figure 4). The composition of the melt progressively evolved with decreasing melt mass, until the crystallization of Fe-Ti oxides and the growth of large clinopyroxene oikocrysts locked the porosity (Stage 3 in Figure 4). This resulted in a random orientation of the crystals and in chemical compositions that follow fractional crystallization trends. Additional processes such as compaction, melt extraction, melt mixing or reactive migration of exotic melts would have caused structural and/or chemical perturbation from the textural and chemical patterns documented in our samples. For example, such complexity has been extensively documented within the lower gabbroic crust from the East Pacific Rise (Hess Deep; e.g., Leuthold et al., 2018; Natland & Dick, 1996) and Southwest Indian Ridge (Atlantis Bank; e.g., Boulanger et al., 2021; Sanfilippo et al., 2020), where a combination of compaction, reactive porous flow and melt replenishment
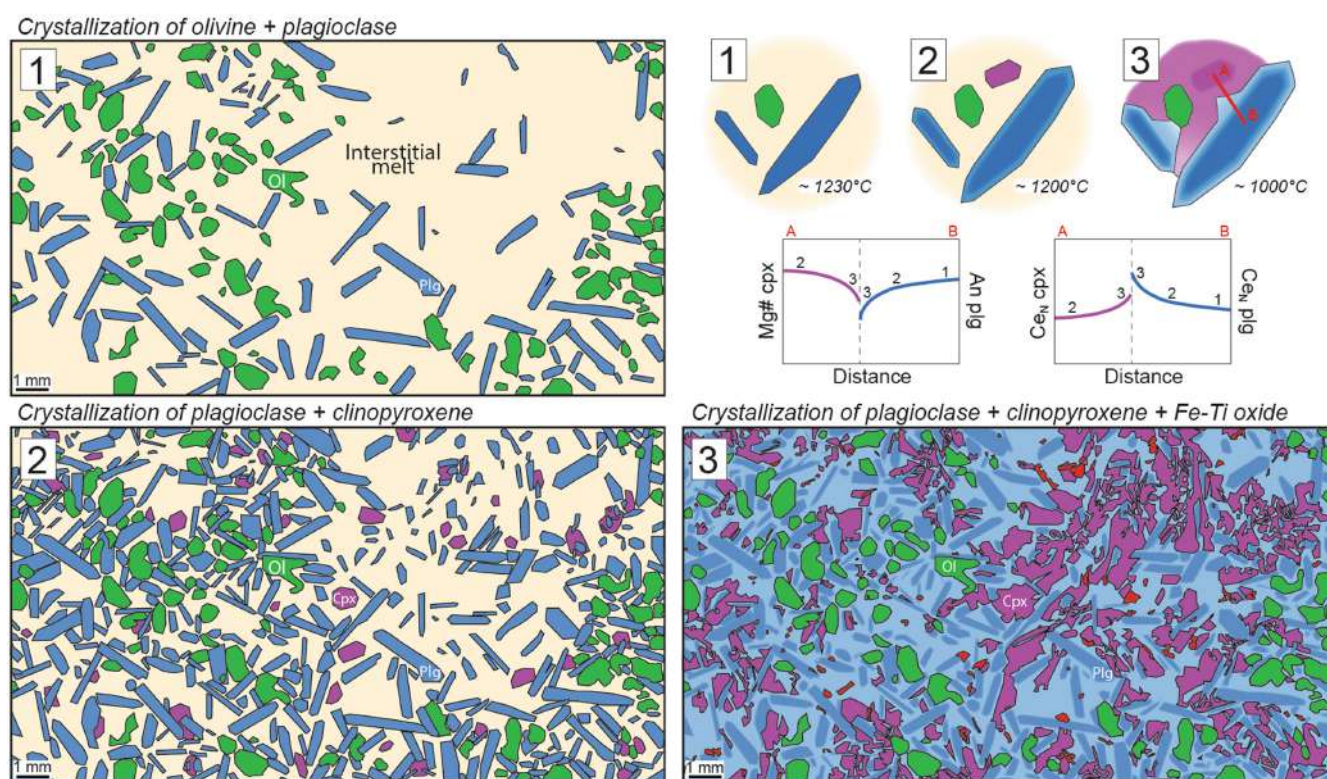

FIGURE 4 Representative evolution of a crystal mush during static crystallization. Stage 1: Heterogeneous crystallization of melt-suspended euhedral olivine and plagioclase. Stage 2: Crystallization of plagioclase and clinopyroxene cores and progressive decrease in porosity. Stage 3: Closure of the porosity at solidus temperatures and formation of plagioclase rims, clinopyroxene oikocrysts and Fe-Ti oxides. Upper right corner: Textural and chemical evolution during cooling and progressive closure of the magmatic system. [Colour figure can be viewed at wileyonlinelibrary.com]

obscured the initial evolution of the crystal mush. We emphasize that such "disturbed" magmatic systems are the rule rather than the exception for oceanic gabbros and the uniqueness of the studied samples stand in their relatively fast and static cooling, which allowed for preservation of the primary texture and chemical composition. This contribution therefore provides a Rosetta stone for deciphering the complexity of the processes occurring in oceanic crystal mushes and implies that any divergence from this reference can be attributed to processes debated in literature, such as dissolution–precipitation, magma mixing and compaction-driven melt extraction.

DATA AVAILABILITY STATEMENT

The data that supports the findings of this study are available in the supplementary material of this article

REFERENCES

Basch, V., Sanfilippo, A., Skolotnev, S. G., Ferrando, C., Muccini, F., Palmiotto, C., Peyve, A. A., Ermolaev, B. V., Okina, O. I., & Ligi, M. (2022). Genesis of oceanic oxide gabbros and gabbronorites during reactive melt migration at transform walls (doldrums Megatransform system; 7-8°N mid-Atlantic ridge). *Journal of Petrology*, 63, 1–23. https://doi.org/10.1093/petrology/egac005

Basch, V., Sanfilippo, A., Vigliotti, L., Langone, A., Rasul, N., Khorsheed, M., AlNomani, S., AlQutub, A., & Ligi, M. (2022). Crustal contamination and hybridization of an embryonic oceanic crust during the Red Sea rifting (Tihama Asir igneous complex, Saudi Arabia). *Journal of Petrology*, 63, 1–23. https://doi.org/10.1093/petrology/egac005

Bertolett, E. M., Prior, D. J., Gravley, D. M., Hampton, S. J., & Kennedy, B. M. (2019). Compacted cumulates revealed by electron backscatter diffraction analysis of plutonic lithics. *Geology*, 47, 445–448. https://doi.org/10.1130/G45616.1

Boulanger, M., France, L., Ferrando, C., Ildefonse, B., Ghosh, B., Sanfilippo, A., Liu, C.-Z., Morishita, T., Koepke, J., & Bruguier, O. (2021). Magma-mush interactions in the lower oceanic crust: Insights from Atlantis Bank layered series (southwest Indian ridge). *Journal of Geophysical Research: Solid Earth*, 126, e2021JB022331. https://doi.org/10.1029/2021JB022331

Cashman, K. V., Sparks, R. S. J., & Blundy, J. D. (2017). Vertically extensive and unstable magmatic systems: A unified view of igneous processes. *Science*, 355, eaag3055. https://doi.org/10.1126/science.aag3055

Cheadle, M. J., & Gee, J. S. (2017). Quantitative textural insights into the formation of gabbro in mafic intrusions. *Elements*, 13, 409–414. https://doi.org/10.2138/gselements.13.6.409

Coogan, L. A., & Dosso, S. E. (2016). Quantifying parental MORB trace element compositions from the eruptive products of realistic magma chambers: Parental EPR MORB are depleted. *Journal of Petrology*, 57, 2105–2126. https://doi.org/10.1093/petrology/egw059

Cooper, K. M. (2017). What does a magma reservoir look like? The 'crystal's-eye' view. *Elements*, 13, 23–28. https://doi.org/10.2113/gselements.13.1.23

Coumans, J. P., Stix, J., Clague, D. A., Minarik, W. G., & Layne, G. D. (2016). Melt-rock interaction near the Moho: Evidence from crystal cargo in lavas from near-ridge seamounts. *Geochimica et Cosmochimica Acta*, 191, 139–164. https://doi.org/10.1016/j.gca.2016.07.017

Dick, H. J. B., Ozawa, K., Meyer, P. S., Niu, Y., Robinson, P. T., Constantin, M., Hebert, R., Maeda, J., Natland, J. H., Hirth, J. G., & Mackie, S. M. (2002). Primary silicate mineral chemistry of a 1.5-km section of very slow spreading lower ocean crust: ODP hole 735B, southwest Indian ridge. In J. H. Natland, H. J. B. Dick, D. J. Miller, & R. P. Von Herzen (Eds.), *Proceedings of the ocean drilling program, scientific results*, Vol. 176 (pp. 1–61). Ocean Drilling Program.

Edmonds, M., Cashman, K. V., Holness, M., & Jackson, M. (2019). Architecture and dynamics of magma reservoirs. *Philosophical Transactions of the Royal Society A*, 377, 20180298. https://doi.org/10.1098/rsta.2018.0298

Feig, S., Koepke, J., & Snow, J. (2006). Effect of water on tholeiitic basalt phase equilibria: An experimental study under oxidizing conditions. *Contributions to Mineralogy and Petrology*, 152, 611–638. https://doi.org/10.1007/s00410-006-0123-2

Ferrando, C., Basch, V., Ildefonse, B., Deans, J., Sanfilippo, A., Barou, F., & France, L. (2021). Role of compaction in melt extraction and accumulation at a slow spreading center: Microstructures of olivine gabbros from the Atlantis Bank (IODP hole U1473A, SWIR). *Tectonophysics*, 815, 229001. https://doi.org/10.1016/j.tecto.2021.229001

Ferrando, C., France, L., Basch, V., Sanfilippo, A., Tribuzio, R., & Boulanger, M. (2021). Grain size variations record segregation of residual melts in slow-spreading oceanic crust (Atlantis Bank, 57°E southwest Indian ridge). *Journal of Geophysical Research: Solid Earth*, 126, e2020JB020997. https://doi.org/10.1029/2020JB020997

Gale, A., Dalton, C. A., Langmuir, C. H., Su, Y., & Schilling, J.-G. (2013). The mean composition of ocean ridge basalts. *Geochemistry, Geophysics, Geosystems*, 14, 489–518. https://doi.org/10.1029/2012GC004334

Ghiorso, M. S., & Sack, O. (1995). Chemical mass transfer in magmatic processes. IV. A revised and internally consistent thermodynamic model for the interpolation and extrapolation of liquid-solid equilibria in magmatic systems at elevated temperatures and pressures. *Contributions to Mineralogy and Petrology*, 119, 197–212. https://doi.org/10.1007/BF00307281

Godard, M., Awaji, S., Hansen, H., Hellebrand, E., Brunelli, D., Johnson, K., Yamasaki, T., Maeda, J., Abratis, M., Christie, D., Kato, Y., Mariet, C., & Rosner, M. (2009). Geochemistry of a long in-situ section of intrusive slow-spread oceanic lithosphere: Results from IODP site U1309 (Atlantis massif, 30°N mid-Atlantic-ridge). *Earth and Planetary Science Letters*, 279, 110–122. https://doi.org/10.1016/j.epsl.2008.12.034

Grove, T. L., Kinzler, R. J., & Brian, W. B. (1992). Fractionation of mid-ocean ridge basalt. In J. P. Morgan, D. K. Blackman, & J. M. Sinton (Eds.), *Mantle flow and generation at mid-ocean ridges*, vol. 71 (pp. 281–311. Geophysical Monograph). American Geophysical Union.

Holness, M. B., Vukmanovic, Z., & Mariani, E. (2017). Assessing the role of compaction in the formation of adcumulates: A microstructural perspective. *Journal of Petrology*, 58, 643–674. https://doi.org/10.1093/petrology/egx037

Ildefonse, B., Arbaret, L., & Diot, H. (1997). Rigid particles in simple shear flow: Is their preferred orientation periodic or steady-state? In J. L. Bouchez, et al. (Eds.), *Granite: From segregation of melt to emplacement fabrics* (pp. 177–185). Kluwer Academic Publishers.

Ildefonse, B., Sokoutis, D., & Mancktelow, N. S. (1992). Mechanical interactions between rigid particles in a deforming ductile matrix. Analogue experiments in simple shear flow. *Journal of Structural Geology, 14*, 1253–1266. https://doi.org/10.1016/0191-8141(92)90074-7

Jackson, M. D., Blundy, J., & Sparks, R. S. J. (2018). Chemical differentiation, cold storage and remobilization of magma in the Earth's crust. *Nature, 564*, 405–409. https://doi.org/10.1038/s41586-018-0746-2

Leuthold, J., Lissenberg, C. J., O'Driscoll, B., Karakas, I., Falloon, T., Klimentyeva, D. N., & Ulmer, P. (2018). Partial melting of lower oceanic crust gabbro: Constraints from poikilitic clinopyroxene primocrysts. *Frontiers in Earth Science, 6*, 15. https://doi.org/10.3389/feart.2018.00015

Lissenberg, C. J., & MacLeod, C. J. (2016). A reactive porous flow control on mid-ocean ridge magmatic evolution. *Journal of Petrology, 57*, 2195–2220. https://doi.org/10.1093/petrology/egw074

Lissenberg, C. J., MacLeod, C. J., & Bennett, E. N. (2019). Consequences of a crystal mush-dominated magma plumbing system: A mid-ocean ridge perspective. *Philosophical Transactions of the Royal Society A, 377*, 20180014. https://doi.org/10.1098/rsta.2018.0014

McKenzie, D. (1984). The generation and compaction of partially molten rock. *Journal of Petrology, 25*(3), 713–765. https://doi.org/10.1093/petrology/25.3.713

Meurer, W. P., & Boudreau, A. E. (1998). Compaction of igneous cumulates part II: Compaction and the development of igneous foliations. *Journal of Geology, 106*, 293–304. https://doi.org/10.1086/516023

Miller, D. J., Abratis, M., Christie, D., Drouin, M., Godard, M., Ildefonse, B., Maeda, J., Weinsteiger, A., Yamasaki, T., Suzuki, Y., Niino, A., Sato, Y., & Takeda, F. (2009). Data report: Microprobe analyses of primary mineral phases from site U1309, Atlantis massif, IODP expedition 304/305. In D. K. Blackman, B. Ildefonse, B. E. John, Y. Ohara, D. J. Miller, C. J. MacLeod, & the Expedition 304/305 Scientists (Eds.), *Proceedings of the International Ocean drilling program 304/305* (p. 4). Integrated Ocean Drilling Program.

Moore, A., Coogan, L. A., Costa, F., & Perfit, M. R. (2014). Primitive melt replenishment and crystal-mush disaggregation in the weeks preceding the 2005–2006 eruption 9°50′N, EPR. *Earth and Planetary Science Letters, 403*, 15–26. https://doi.org/10.1016/j.epsl.2014.06.015

Namur, O., Humphreys, M. C. S., & Holness, M. B. (2013). Lateral reactive infiltration in a vertical gabbroic crystal mush, skaergaard intrusion, east greenland. *Journal of Petrology, 54*(5), 985–1016. https://doi.org/10.1093/petrology/egt003

Natland, J. H., & Dick, H. J. B. (1996). Melt migration through high-level gabbroic cumulates of the East Pacific Rise at Hess Deep: The origin of magma lenses and the deep crustal structure of fast-spreading ridges. *Proceedings of the Ocean Drilling Program*. https://doi.org/10.2973/odp.proc.sr.147.002.1996

Sanfilippo, A., MacLeod, C. J., Tribuzio, R., Lissenberg, C. J., & Zanetti, A. (2020). Early-stage melt-rock reaction in a cooling crystal mush beneath a slow-spreading mid-ocean ridge (IODP hole U1473A, Atlantis Bank, southwest Indian ridge). *Frontiers in Earth Science, 8*, 579138. https://doi.org/10.3389/feart.2020.579138

Skolotnev, S. G., Sanfilippo, A., Peyve, A. A., Muccini, F., Sokolov, S. Y., Sani, C., Dobroliubova, K. O., Ferrando, C., Chamov, N. P., Palmiotto, C., Pertsev, A. N., Bonatti, E., Cuffaro, M., Gryaznova, A. C., Sholukhov, K. N., Bich, A. S., & Ligi, M. (2020). Large-scale structure of the doldrums multi-fault transform system (7-8°N equatorial Atlantic): Preliminary results from the 45th expedition of the R/V a.N. Strakhov. *Ofioliti, 45*, 25–41.

Smith, R. K., & Lofgren, G. E. (1983). An analytical and experimental study of zoning in plagioclase. *Lithos, 16*, 153–168.

Sparks, R. S. J., Annen, C., Blundy, J. D., Cashman, K. V., Rust, A. C., & Jackson, M. D. (2019). Formation and dynamics of magma reservoirs. *Philosophical Transactions of the Royal Society A, 377*, 20180019. https://doi.org/10.1098/rsta.2018.0019

Sun, S. S., & McDonough, W. F. (1989). Chemical and isotopic systematics of oceanic basalts: Implications for mantle composition and processes. *Geological Society of London, Special Publications, 42*, 313–345. https://doi.org/10.1144/GSL.SP.1989.042.01.19

Tegner, C., Thy, P., Holness, M. B., Jakobsen, J. K., & Lesher, C. E. (2009). Differentiation and compaction in the Skaergaard intrusion. *Journal of Petrology, 50*, 813–840. https://doi.org/10.1093/petrology/egp020

Villiger, S., Ulmer, P., & Müntener, O. (2007). Equilibrium and fractional crystallization experiments at 0.7 GPa: The effect of pressure on phase relations and liquid compositions of tholeiitic magmas. *Journal of Petrology, 48*, 159–184. https://doi.org/10.1093/petrology/egl058

White, R. S., Edmonds, M., Maclennan, J., Greenfield, T., & Agustsdottir, T. (2019). Melt movement through the Icelandic crust. *Philosophical Transactions of the Royal Society A, 377*, 20180010. https://doi.org/10.1098/rsta.2018.0010

Workman, R. K., & Hart, S. R. (2005). Major and trace element composition of the depleted MORB mantle (DMM). *Earth and Planetary Science Letters, 231*, 53–72. https://doi.org/10.1016/j.epsl.2004.12.005

Zhang, W.-Q., Liu, C.-Z., & Dick, H. J. B. (2020). Evidence for multi-stage melt transport in the lower ocean crust: The atlantis bank gabbroic massif (IODP Hole U1473A, SW Indian Ridge). *Journal of Petrology, 61*(9). https://doi.org/10.1093/petrology/egaa082

SUPPORTING INFORMATION

Additional supporting information can be found online in the Supporting Information section at the end of this article.